# Aerodynamic Behavior of the Viking Entry Vehicle: Ground Test and Flight Results

Donn B. Kirk,* Peter F. Intrieri,* and Alvin Seiff†
*NASA Ames Research Center, Moffett Field, Calif.*

**An extensive series of tests of the Viking entry vehicle flying in pure $CO_2$ was conducted in a ballistic range at Ames Research Center. The primary purpose of these tests was to calibrate the aerodynamic lift and drag characteristics in order to allow the density, pressure, and temperature profiles of the Martian atmosphere to be determined from onboard instrumentation carried on Viking. Both the Viking 1 and Viking 2 entry vehicles performed flawlessly during entry and descent, and the atmosphere structure was deduced to an altitude of about 120 km. A description is given of the ballistic range tests and of the aerodynamic behavior of the full-scale entry vehicles during entry into the Martian atmosphere. Some comparisons between ground test and flight results are shown.**

## Introduction

ON July 20, 1976, the Viking 1 spacecraft entered the atmosphere of Mars and made a soft landing on the surface of the planet. On September 3, Viking 2 achieved similar success. During these entries, which lasted approximately 9 minutes each, measurements were made to determine the physical and chemical properties of the Martian atmosphere. The success of these measurements and, indeed, the success of the landings, depended on the aerodynamic behavior of the lifting entry vehicle, which had to provide a smooth stable descent through the very thin atmosphere. In addition, there was a requirement that the vehicle aerodynamics be known very precisely to allow the density, pressure, and temperature of the Martian atmosphere to be deduced from onboard deceleration measurements.[1-3] The purpose of this paper is to describe the aerodynamic behavior experienced by the Viking entry vehicles during descent through the Martian atmosphere and to make comparisons where possible with ground test data.

## Ground Test Data

The Viking entry vehicle is shown in Fig. 1. The forebody is basically a blunt-nosed 70-deg half-angle cone with a ratio of nose radius to base radius of 0.5. The center of gravity was offset from the axis of symmetry to make it a lifting configuration ($z_{cg}/d = 0.0134$, $L/D \cong 0.18$). The nominal preflight Viking entry trajectory is shown in Fig. 2, where Reynolds number based on body diameter is plotted versus velocity. The entry velocity was nominally 4.6 km/s. The circles indicate conditions where ground data were obtained, matching a number of points along the nominal trajectory. The data were obtained in the Ames Hypersonic Free Flight Aerodynamic Facility, a ballistic range with 16 shadowgraph stations evenly spaced over the 23-m test section. Models with diameters of 1.02 and 2.03 cm were launched into flight from deformable-piston light-gas guns with bore diameters of 1.27 and 2.54 cm. Photographic data giving the time history of the model attitude and position were obtained from the 16 pairs of orthogonal shadowgraph stations, each of which is spark illuminated and Kerr cell shuttered to produce an exposure time of only $30 \times 10^{-9}$ s. The timing information was recorded by sixteen 100-MHz counters activated by signals from the Kerr cell shutters. The aerodynamic characteristics (lift, drag, static and dynamic stability, and trim angle of attack) were determined by analyzing the free-flight motions using data reduction programs described in Refs. 4 and 5.

Because gas properties can significantly affect the aerodynamics of probe configurations,[6] the tests were conducted in an essentially 100% $CO_2$ atmosphere, which was believed to be characteristic of the Martian atmosphere (confirmed by Viking 1 results[7]). This is demonstrated in Fig. 3, where Viking drag data in $CO_2$ and air at one Reynolds-number/velocity condition are compared. The variation with angle of attack is similar in the two gases, but the drag level is higher in $CO_2$. Errors in drag coefficient would lead directly to errors in the deduced Martian atmospheric density and pressure. A very large and potentially significant difference in vehicle aerodynamics is shown in Fig. 4, where the static stability parameter $C_{m_\alpha}$ is plotted against angle of attack. The carbon dioxide data show large nonlinearity with angle of attack and indicate a static instability at small angles of attack. The air data show a large and essentially constant stability level at all angles of attack.

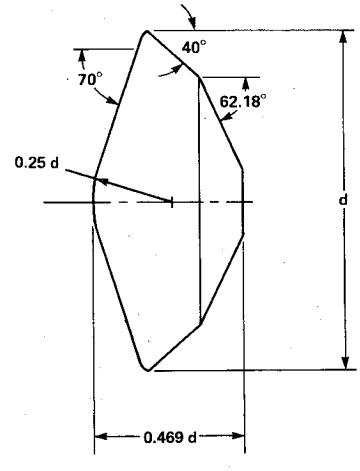


**Fig. 1 Sketch of Viking entry vehicle.**

Presented as Paper 77-1160 at the AIAA 4th Atmospheric Flight Mechanics Conference, Hollywood, Fla., Aug. 8-10, 1977; submitted Sept. 8, 1977; revision received Feb. 1, 1978. 

Index categories: Entry Vehicle Testing, Flight and Ground; Entry Vehicle Dynamics and Control.

*Research Scientist.
†Staff Scientist. Associate Fellow AIAA.

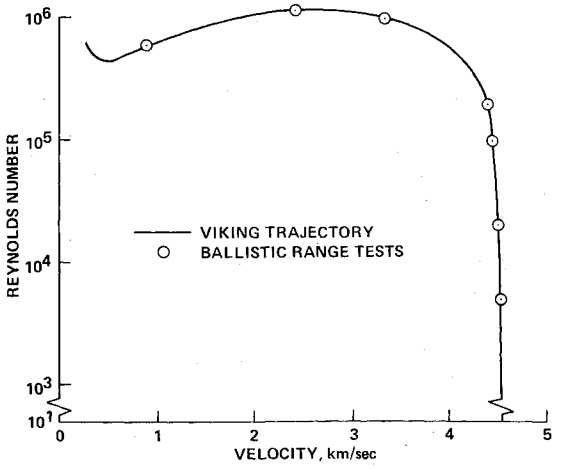


Fig. 2 Nominal Viking entry trajectory.

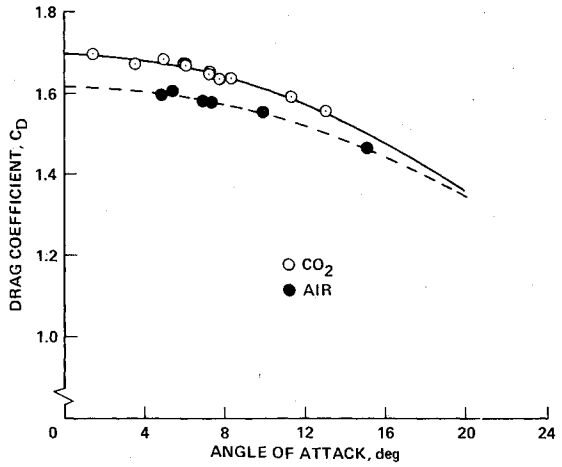


Fig. 3 Effect of gas composition on Viking drag coefficient: $V=3.4$ km/s, $Re=0.8\times10^6$.

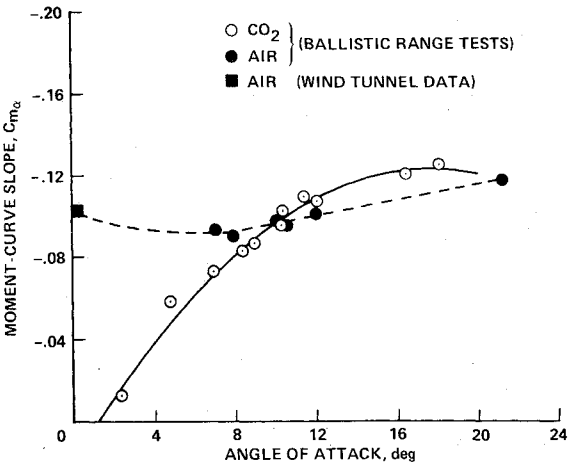


Fig. 4 Effect of gas composition on Viking static stability: $V=3.4$ km/s, $Re=0.8\times10^6$.

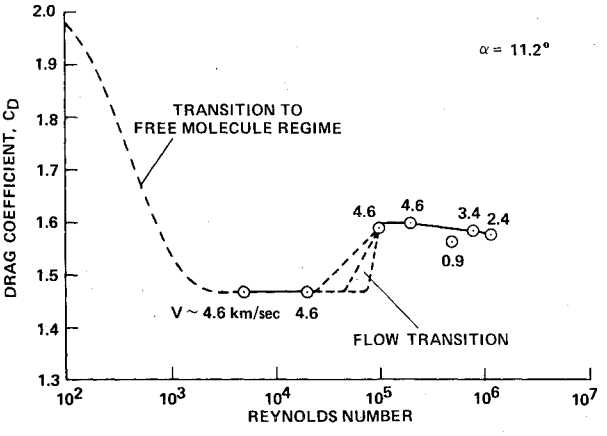


Fig. 5 Effect of Reynolds number on Viking drag coefficient.

Figure 5 shows the drag data from the ballistic range tests plotted versus Reynolds number. Over the high Reynolds number flight regime ($Re>10^5$), the drag coefficient is nearly constant at a value near 1.6. Just below a Reynolds number of $10^5$, a significantly smaller drag coefficient was measured and three alternative fairings to reach this level are indicated with dashes. It was first assumed that this drag difference was a consequence of boundary-layer transition from laminar to turbulent; however, a more detailed analysis indicates that the difference is likely due to a transition from nonequilibrium to equilibrium flow in the shock layer (see Appendix). Another region which is shown with dashes lies below the lowest test Reynolds number, where $C_D$ was modeled after the drag variation seen in low Reynolds number tests of spheres.[8] The increase in drag coefficient occurs as slip flow and then free-molecule flow are obtained. Additional ballistic range tests, undertaken recently and not yet completed, have confirmed this effect for the Viking geometry.

## Flight Results

The aerodynamic behaviors of Viking 1 and 2 were essentially identical; the authors have arbitrarily chosen flight data from one or the other for presentation herein. Figure 6 shows the axial deceleration pulse experienced by Viking 2 as measured by an onboard accelerometer, indicating a peak of about 73 m/s$^2$. The sampling rate was 10/s and the data were transmitted as velocity pulse counts; these data were extremely accurate, one pulse denoting a velocity decrease of only 1.3 cm/s. Analysis of this deceleration history and those

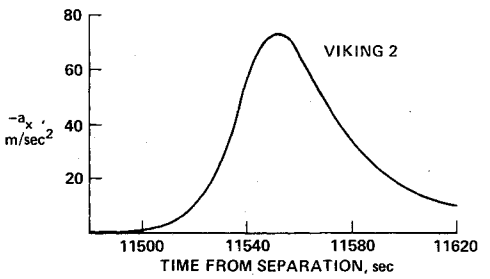


Fig. 6 Viking 2 axial deceleration pulse.

from orthogonal accelerometers, together with the ground-determined aerodynamics, yielded the density, pressure, and temperature of the Martian atmosphere up to about 120 km altitude. To any reasonable scale, this deceleration curve looks absolutely smooth, but if successive differences in deceleration are plotted versus time, an interesting result is observed. This is shown in Fig. 7. The differences vary smoothly for a while, change character for about 10 s, and then are relatively smooth for the remainder of the entry. The erratic period encompasses a Reynolds number range from about 80,000 to 180,000. This same phenomenon at about the same Reynolds number also occurred during the Viking 1 entry. Because of the correspondence in Reynolds number, it is postulated that we are seeing flight evidence of non-equilibrium to equilibrium flow transition similar to that which caused the step change in $C_D$ shown in Fig. 5.

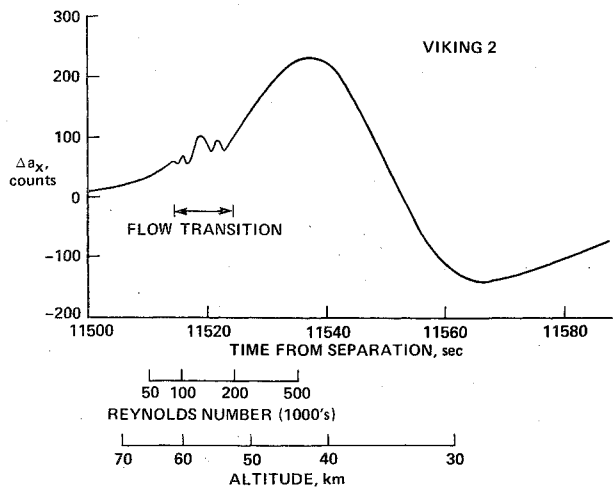


Fig. 7 Indication of nonequilibrium to equilibrium flow transition for Viking 2.

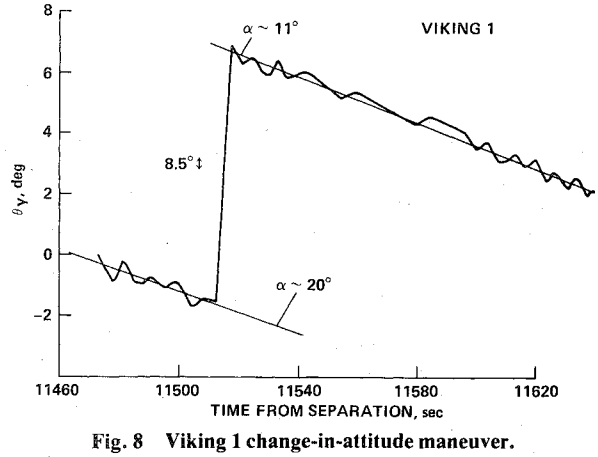


Fig. 8 Viking 1 change-in-attitude maneuver.

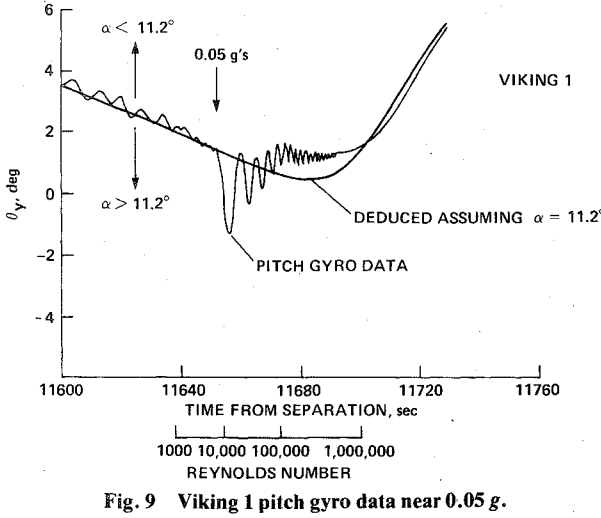


Fig. 9 Viking 1 pitch gyro data near 0.05 $g$.

Figure 8 shows the pitch gyro data from Viking 1 during the time when it went through a maneuver to orient for atmospheric entry. Before $t = 11{,}513$ s, the entry vehicle was programmed to maintain a constant angle of attack of approximately 20 deg, as required for data collection by the onboard retarding potential analyzer. Thrusters were fired to maintain this angle of attack and this is the reason for the irregularity of the data. The data indicated a steady decrease of pitch angle with time because the trajectory was being bent

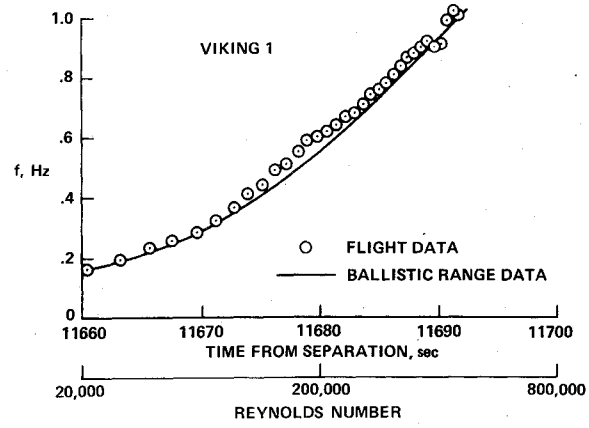


Fig. 10 Frequency comparison between ballistic range data and Viking 1 flight results.

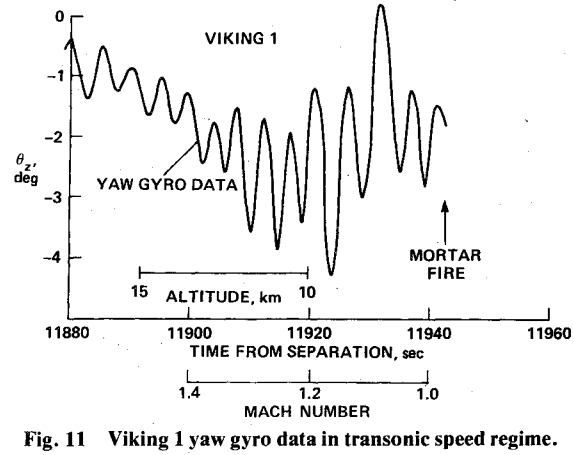


Fig. 11 Viking 1 yaw gyro data in transonic speed regime.

due to gravitational attraction. At $t = 11{,}513$ s, an onboard clock indicated that the vehicle had reached its "entry" altitude of 244 km, at which time it was programmed to orient itself at its nominal trim angle of attack (about 11 deg) and maintain this attitude until sensing 0.05 $g$ deceleration. Figure 8 shows that in about 5 s the vehicle attitude changed by 8.5 deg, exactly as programmed, and the new angle of attack was maintained within a few tenths of a degree.

Figure 9 continues this pitch gyro data later in time. At $t = 11{,}653$ s (altitude about 80 km), the onboard axial accelerometer detected 0.05 $g$ and the vehicle was freed to seek its aerodynamic trim angle of attack. The smooth curve on this figure is a computer analysis of the trajectory, which assumes the angle of attack was constant at 11.2 deg (the trim angle deduced from the ballistic range tests), and it is seen that the flight data indicate the first few oscillations were at a slightly higher angle, then about half a degree lower, and finally very close to the expected trim. The change in trim angle of attack from 11,653 to 11,670 s is attributed to the change in the flow from nonequilibrium to equilibrium (see Appendix).

Measurable oscillations in the angle of attack lasted about 40 s, while the vehicle descended from 80 to 43 km, after which the oscillation amplitudes were negligible. About 15 oscillations with amplitudes greater than about 0.1 deg were experienced. Figure 10 compares the frequency of these oscillations with that predicted from the ground-based data. The agreement is excellent.

Figure 11 shows the yaw gyro data from Viking 1 late in the trajectory. The time of mortar fire is indicated, shortly after which a parachute was deployed. The Mach number at mortar fire was about 1, and the ground-based data indicated that the Viking was dynamically unstable in the transonic speed

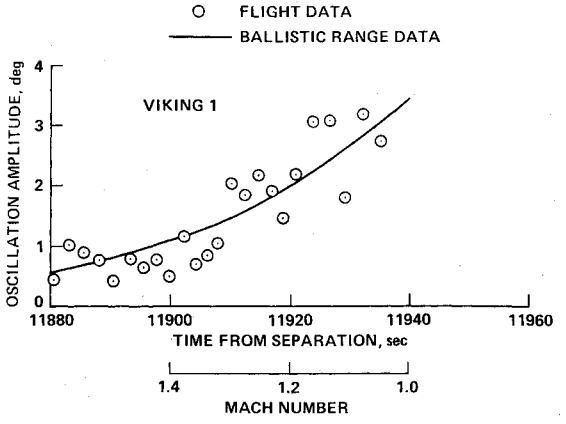


**Fig. 12 Amplitude comparison between ballistic range data and Viking 1 flight results.**

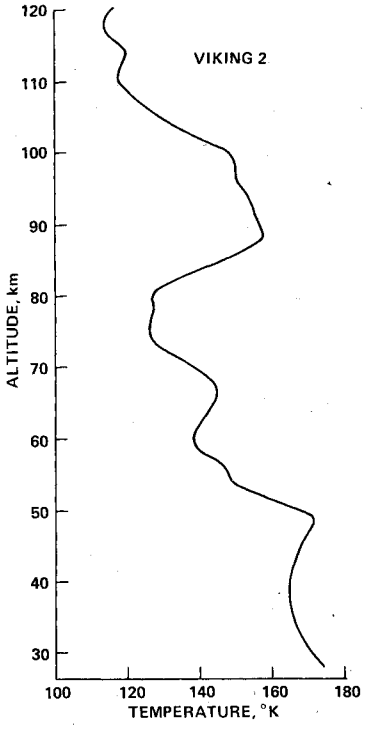


**Fig. 13 Temperature profile of Mars' atmosphere deduced from Viking 2 deceleration measurements.**

regime. A significant growth in the oscillation amplitude is indicated in Fig. 11. Figure 12 shows this oscillation amplitude as a function of time and Mach number and compares it to that predicted by the ballistic range results. The onboard reaction control system fired a number of times during this period in an attempt to limit the yaw rate. This probably accounts for the scatter in the flight data. Although dynamic stability is one of the most difficult aerodynamic characteristics to determine in ground-based facilities, the data show overall good agreement with the flight results.

The ultimate use for all the aerodynamic data obtained in the ballistic range tests was the determination of the density, pressure, and temperature of the Martian atmosphere as functions of altitude. This aspect of the results has been discussed in detail in other publications.[9,10] The onboard accelerometer data allowed the atmospheric density to be determined down to a level of $10^{-8}$ kg/m$^3$, and the pressure down to $10^{-5}$ mbar. The most dramatic result obtained for the three state properties, however, was the temperature. The temperature profile from the Viking 2 accelerometry is shown in Fig. 13 (reproduced from Ref. 9). The pronounced waviness in the temperature structure is attributed to a diurnal thermal tide in the atmosphere of Mars,[9] a possibility which had been studied by Zurek[11] and others before the Viking entries. Viking 1 results, which were at a lower latitude, showed a similar wavy structure in the temperature profile.[6,9] The precise knowledge of the Viking aerodynamics from the ballistic range results allows confidence to be placed in the temperature profiles.

## Conclusions

Both the Viking 1 and Viking 2 entry vehicles performed flawlessly during Martian entry. The flight behavior was fully consistent with expectations based on tests conducted in $CO_2$. The aerodynamic data obtained in the ballistic range tests agreed with the flight data very closely and allowed the structure of the Martian atmosphere to be determined to an altitude above 100 km.

## Appendix

The reason for the drop in drag coefficient at a Reynolds number of about $10^5$ has been a puzzle. At first it was thought to be due to boundary-layer transition in the wake, since changes in $C_D$ with Reynolds number are frequently associated with boundary-layer transition. The argument can be made, based on past test data, that when the wake goes laminar, wake convergence decreases and causes the base pressure to increase and $C_D$ to decrease, consistent with the data shown in Fig. 5. This explanation was countered, however, by examination of the base pressures measured during the Viking entries into Mars' atmosphere. In the altitude range from 50 to 60 km, no evidence of a step change was seen in the base pressure, and the magnitude of base pressure ($p_b/p_\infty \simeq 7$) was insufficient to support the observed change in $C_D$. An alternate explanation was sought.

Could the drag change result from onset of nonequilibrium flow effects in the shock layer? In Ref. 12, Hindelang modeled nonequilibrium flow behind a normal shock wave in $CO_2$ at freestream velocities of 5 and 2.5 km/s. His numerical calculations of the nonequilibrium zone at 5 km/s can be represented by the binary scaling expression $xp_\infty = 6 \times 10^{-4}$ cm-atm, where $x$ is the length of flow required to come within about 0.9 of equilibrium mass density. (At 2.5 km/s, $xp_\infty = 12.5 \times 10^{-4}$ cm-atm.) These expressions would predict $x/r_b = 0.08$, 0.34, and 1.36 for the ballistic range tests at $Re = 10^5$, $2 \times 10^4$, and $5 \times 10^3$, respectively, implying a transition from equilibrium (values of $x/r_b$ near zero) to nonequilibrium flow in this Reynolds number range. Similarly, in the flight data between 63 and 52 km (the nonsmooth region shown in Fig. 7), $x/r_b$ varies between about 0.71 and 0.16, again suggesting the transition region.

The Viking forebody is particularly sensitive to nonequilibrium flow, because the bow shock wave is on the borderline between attached conical-type flow and detached curved-bow-shock blunt body flow. Shadowgraphs from the ballistic range tests show that a transition between these two flow types does occur on the leeward side of the forebody at the trim angle of attack as Reynolds number is reduced. The change in flow configuration can be regarded as a result of change in the ratio of specific heats when the gas is, or is not, in equilibrium. This change in flow configuration is believed responsible for the observed change in drag coefficient.

## References

[1] Seiff, A. and Reese, D. E., "Defining Mars' Atmosphere – a Goal for Early Missions," *Astronautics and Aeronautics*, Vol. 3, Feb. 1965, pp. 16-21.

[2] Peterson, V. L., "A Technique for Determining Planetary Atmosphere Structures from Measured Accelerations of an Entry Vehicle," NASA TN D-2669, 1965.

[3] Seiff, A., Reese, D. E., Sommer, S. C., Kirk, D. B., Whiting, E. E., and Niemann, H. B., "PAET, an Entry Probe Experiment in the Earth's Atmosphere," *Icarus*, Vol. 18, April 1973, pp. 525-563.

[4]Malcolm, G. N. and Chapman, G. T., "A Computer Program for Systematically Analyzing Free-Flight Data to Determine the Aerodynamics of Axisymmetric Bodies," NASA TN D-4766, 1968.

[5]Canning, T. N., Seiff, A., and James, C. S. (eds.), "Ballistic Range Technology," AGARDograph 138, Aug. 1970.

[6]Intrieri, P. F., DeRose, C. E., and Kirk, D. B., "Flight Characteristics of Probes in the Atmospheres of Mars, Venus, and the Outer Planets," *Acta Astronautica*, Vol. 4, July-Aug. 1977, pp. 789-799.

[7]Nier, A. O., et al., "Composition and Structure of the Martian Atmosphere: Preliminary Results From Viking 1," *Science*, Vol. 193, Aug. 1976, pp. 786-788.

[8]Masson, D. J., Morris, D. N., and Bloxsom, D. E., in *Rarified Gas Dynamics*, edited by L. Talbot, Academic Press, New York, 1961, p. 643.

[9]Seiff, A. and Kirk, D. B., "Structure of the Atmosphere of Mars in Summer at Midlatitudes," *Journal of Geophysical Research*, Vol. 82, Sept. 1977, pp. 4364-4378.

[10]Seiff, A. and Kirk, D. B., "Structure of Mars' Atmosphere up to 100 Kilometers from the Entry Measurements of Viking 2," *Science*, Vol. 194, Dec. 1976, pp. 1300-1303.

[11]Zurek, R. W., "Diurnal Tide in the Martian Atmosphere," *Journal of Atmospheric Science*, Vol. 33, Feb. 1976, pp. 321-337.

[12]Hindelang, F. J., "Coupled Vibration and Dissociation Relaxation Behind Strong Shock Waves in Carbon Dioxide," NASA TR R-253, 1967.